Phase transitions in the sdg interacting boson model

P. Van Isacker, A. Bouldjedri, S. Zerguine

Phase transitions in the sdg interacting boson model

P Van Isacker†, A Bouldjedri‡ and S Zerguine‡

† Grand Accélérateur National d'Ions Lourds, CEA/DSM–CNRS/IN2P3, BP 55027, F-14076 Caen Cedex 5, France

‡ Department of Physics, PRIMALAB Laboratory, University of Batna, Avenue Boukhelouf M El Hadi, 05000 Batna, Algeria

Abstract. A geometric analysis of the sdg interacting boson model is performed. A coherent-state is used in terms of three types of deformation: axial quadrupole (β_2), axial hexadecapole (β_4) and triaxial (γ_2). The phase-transitional structure is established for a schematic sdg hamiltonian which is intermediate between four dynamical symmetries of U(15), namely the spherical U(5) $\otimes$ U(9), the (prolate and oblate) deformed SU$_\pm$(3) and the γ_2-soft SO(15) limits. For realistic choices of the hamiltonian parameters the resulting phase diagram has properties close to what is obtained in the sd version of the model and, in particular, no transition towards a stable triaxial shape is found.

1. Introduction

Phase transitions are well-known phenomena. They are said to occur if an order parameter of the system experiences, as function of a control parameter, a rapid change at a particular point. A phase transition may be of first or second order, depending on the discontinuity of the first- or second-order derivative of the order parameter as a function of the control parameter (Ehrenfest classification). Phase transitions have been observed in countless classical and quantal systems, usually composed of very large numbers of particles and hence allowing a statistical treatment. The atomic nucleus, however, consists of less than 300 particles (nucleons) and finite-system effects may therefore play a role.

The concept of phase transitions is used in nuclear physics either to describe the behaviour of hot nuclei resulting from heavy-ion collisions or in the context of so-called 'quantum' phase transitions, also called shape phase transitions. The latter is the subject this paper and relies on a method proposed by Gilmore in 1979 [1]. Its central idea is that any quantum-mechanical hamiltonian that can be written in terms of the generators of a compact Lie algebra, has an unambiguously defined classical analogue with a geometric interpretation in terms of shape variables of which the phase-transitional behaviour can be studied. A few years before Gilmore's proposal, in the middle of the 1970s, Arima and Iachello [2, 3, 4, 5] had proposed a novel way to describe the nucleus with a set of s and d bosons, called the interacting boson model (IBM) [6], which precisely has the

property that it can be cast in terms of generators of the unitary Lie algebra U(6) to which Gilmore's technique can be applied. This approach was advocated by Dieperink *et al.* [7] and lead to a geometric interpretation of the IBM [8, 9] and to a connection with the Bohr–Mottelson description of the nucleus [10]. The problem of phase transitions in the IBM was subsequently addressed by Feng *et al.* [11] but was solved in its full generality only many years later by López-Moreno and Castaños [12].

Although the early work in the 1980s determined the most essential phase-transitional properties of the IBM, many additional related features of the model have been studied over the years [13, 14, 15]. This area of research received renewed impetus following Iachello's suggestion of critical-point symmetries E(5) and X(5) [16, 17], nuclear examples of which were proposed by Casten and Zamfir [18, 19]. The central idea of Iachello's method is to provide a description of nuclei at the phase-transitional point through the (approximate) analytic solution of a geometric Bohr hamiltonian. This rekindled interest in the phase-transitional behaviour of algebraic models from various angles: the correspondence between the E(5) solution of the Bohr hamiltonian and the U(5)–SO(6) transition in the IBM was studied in detail [20, 21, 22, 23, 24], the existence of an additional prolate–oblate transition was recognized [25, 26], a connection with Landau theory of phase transitions was established [27, 28, 29], the influence of angular momentum was investigated [30, 31, 32], the connection with shape coexistence was revisited [33], the algebraic framework of quasi-dynamical symmetries was established to deal with transitions between two phases [34, 35, 36, 37, 38], phase transitions of excited states were considered [39]. In addition, several extensions of the IBM were re-examined from this angle such as the neutron–proton version of the model [40] or its configuration-mixed version [41].

In this paper we report on a phase-transitional study of another extension of the IBM, namely the *sdg*-IBM, which includes a *g* boson to account for hexadecapole deformations of the nucleus. We give a brief review of the *sdg*-IBM in section 2 and discuss its classical limit in section 3. Since a general *sdg* hamiltonian has too many interaction parameters, a simpler parametrization is proposed in section 4. The method for establishing the phase diagram is explained in section 5 for the specific case of the *sdg*-IBM and then applied to obtain partial and complete diagrams in sections 6 and 7, respectively. The conclusions of this work are summarized in section 8.

2. The general hamiltonian of *sdg*-IBM

We refer the reader to the paper of Devi and Kota [42] for an excellent review of studies with the *sdg*-IBM. We limit ourselves here to a concise description of the hamiltonian of the model which is needed in this work. The building blocks of the *sdg*-IBM are s, d and g bosons with angular momenta $\ell = 0$, 2 and 4. A nucleus is characterized by a constant total number of bosons N which equals half the number of valence nucleons (particles or holes, whichever is smaller). No distinction is made here between neutron and proton bosons.

Since the hamiltonian of the *sdg*-IBM conserves the total number of bosons, it can be written in terms of the 225 operators $b_{\ell m}^{\dagger} b_{\ell' m'}$ where $b_{\ell m}^{\dagger}$ ($b_{\ell m}$) creates (annihilates) a boson with angular momentum ℓ and z projection m. This set of 225 operators generates the Lie algebra U(15) of unitary transformations in fifteen dimensions. A hamiltonian that conserves the total number of bosons is of the generic form

$$\hat{H} = E_0 + \hat{H}^{(1)} + \hat{H}^{(2)} + \cdots, \tag{1}$$

where the index refers to the order of the interaction in the generators of U(15). The first term E_0 is a constant which represents the binding energy of the core. The second term is the one-body part

$$\hat{H}^{(1)} = \epsilon_s [s^{\dagger} \times \tilde{s}]^{(0)} + \epsilon_d \sqrt{5} [d^{\dagger} \times \tilde{d}]^{(0)} + \epsilon_g \sqrt{9} [g^{\dagger} \times \tilde{g}]^{(0)}$$
$$\equiv \epsilon_s \hat{n}_s + \epsilon_s \hat{n}_d + \epsilon_d \hat{n}_g, \tag{2}$$

where $\times$ refers to coupling in angular momentum (shown as an upperscript in round brackets), $\tilde{b}_{\ell m} \equiv (-)^{\ell-m} b_{\ell,-m}$ and the coefficients ϵ_s, ϵ_d and ϵ_g are the energies of the s, d and g bosons, respectively. The third term in the hamiltonian (1) represents the two-body interaction

$$\hat{H}^{(2)} = \sum_{\ell_1 \leq \ell_2, \ell_1' \leq \ell_2', L} \tilde{v}_{\ell_1 \ell_2 \ell_1' \ell_2'}^{L} [[b_{\ell_1}^{\dagger} \times b_{\ell_2}^{\dagger}]^{(L)} \times [\tilde{b}_{\ell_2'} \times \tilde{b}_{\ell_1'}]^{(L)}]_0^{(0)}, \tag{3}$$

where the coefficients $\tilde{v}$ are related to the interaction matrix elements between normalized two-boson states,

$$\tilde{v}_{\ell_1 \ell_2 \ell_1' \ell_2'}^{L} = \sqrt{\frac{2L+1}{(1+\delta_{\ell_1 \ell_2})(1+\delta_{\ell_1' \ell_2'})}} \langle \ell_1 \ell_2; LM | \hat{H}^{(2)} | \ell_1' \ell_2'; LM \rangle. \tag{4}$$

Since the bosons are necessarily symmetrically coupled, allowed two-boson states are s^2 ($L = 0$), sd ($L = 2$), sg ($L = 4$), d^2 ($L = 0, 2, 4$), dg ($L = 2, 3, 4, 5, 6$) and g^2 ($L = 0, 2, 4, 6, 8$). Since for n states with a given angular momentum one has $n(n+1)/2$ interactions, 32 independent two-body interactions v are found: six for $L = 0$, ten for $L = 2$, one for $L = 3$, ten for $L = 4$, one for $L = 5$, three for $L = 6$ and one for $L = 8$. Together with the constant E_0 and the three single-boson energies ϵ_s, ϵ_d and ϵ_g, a total of 36 parameters is thus needed to specify completely the hamiltonian of the *sdg*-IBM which includes up to two-body interactions. This number is far too great for practical applications. In the following sections we explain how possible simplifications draw inspiration from the classical limit and from the *sd*-IBM.

3. The classical limit

The classical limit of an IBM hamiltonian is defined as its expectation value in a coherent state [1] and yields a function of the relevant deformation parameters which can be interpreted as a potential surface depending on these parameters. The method was first proposed for the *sd*-IBM [8, 7, 9]. The extension to the *sdg*-IBM was carried out by Devi and Kota [43] who established the classical limit of the various limits of U(15).

The coherent state for the *sdg*-IBM is given by

$$|N; \alpha_{2\mu}, \alpha_{4\mu}\rangle \propto \left(s^\dagger + \sum_\mu \alpha_{2\mu} d_\mu^\dagger + \sum_\mu \alpha_{4\mu} g_\mu^\dagger \right)^N |o\rangle, \tag{5}$$

where $|o\rangle$ is the boson vacuum and the $\alpha_{\lambda\mu}$ are the spherical tensors of quadrupole ($\lambda = 2$) and hexadecapole ($\lambda = 4$) deformation. They have the interpretation of shape variables and their associated conjugate momenta. If one limits oneself to static problems, the $\alpha_{\lambda\mu}$ can be taken as real; they specify a shape and are analogous to the shape variables of the droplet model of the nucleus [10]. In particular, they satisfy the same constraints as the latter which follow from reflection symmetry, that is, (i) $\alpha_{\lambda\mu} = \alpha_{\lambda-\mu}$ and (ii) $\alpha_{\lambda\mu} = 0$ for μ odd.

The most general parametrization of a surface with quadrupole and hexadecapole deformation has been discussed by Rohoziński and Sobiczewski [44] and involves five shape parameters: two of quadrupole (β_2 and γ_2) and three of hexadecapole character (β_4, γ_4 and δ_4). A considerable simplification of the problem is obtained by relating the two hexadecapole variables (γ_4 and δ_4) that parametrize deviations from axial symmetry in terms of the corresponding quadrupole variable γ_2, according to the Cayley-Hamilton theorem [45]. In terms of the latter variables, the coherent state (5) is rewritten as

$$
\begin{aligned}
|N; \beta_2, \beta_4, \gamma_2\rangle = {} & \sqrt{\frac{1}{N!(1+\beta_2^2+\beta_4^2)^N}} \\
& \times \Big(s^\dagger + \beta_2 \big[\cos\gamma_2 d_0^\dagger + \sqrt{\tfrac{1}{2}} \sin\gamma_2 (d_{-2}^\dagger + d_{+2}^\dagger) \big] \\
& + \tfrac{1}{6}\beta_4 \big[(5\cos^2\gamma_2 + 1)g_0^\dagger + \sqrt{\tfrac{15}{2}} \sin 2\gamma_2 (g_{-2}^\dagger + g_{+2}^\dagger) \\
& + \sqrt{\tfrac{35}{2}} \sin^2\gamma_2 (g_{-4}^\dagger + g_{+4}^\dagger) \big] \Big)^N |o\rangle.
\end{aligned}
\tag{6}
$$

The range of allowed values for the quadrupole shape variables is $0 \leq \beta_2 < +\infty$ and $0 \leq \gamma_2 \leq \pi/3$. On the other hand, the hexadecapole shape variable β_4 is unrestricted [45]. The expectation value of the hamiltonian (1) in this state can be determined by elementary methods [46] and yields a function of β_2, β_4 and γ_2 which is identified with a potential $V(\beta_2, \beta_4, \gamma_2)$. In this way the classical limit of the hamiltonian (1) has the following generic form:

$$
\begin{aligned}
V(\beta_2, \beta_4, \gamma_2) = {} & E_0 + \sum_{n \geq 1} \frac{N(N-1)\cdots(N-n+1)}{(1+\beta_2^2+\beta_4^2)^n} \\
& \times \sum_{klm} a_{kl;m}^{(n)} (\beta_2)^k (\beta_4)^l \cos(3m\gamma_2),
\end{aligned}
\tag{7}
$$

where n refers to the order of the interaction. If up to two-body terms are included in the hamiltonian, the non-zero coefficients $a_{kl;m}^{(n)}$ are

$$a_{00;0}^{(1)} = \epsilon_s, \quad a_{20;0}^{(1)} = \epsilon_d, \quad a_{02;0}^{(1)} = \epsilon_g,$$

$$a_{00;0}^{(2)} = \tfrac{1}{2}v_{ssss}^0, \quad a_{20;0}^{(2)} = \sqrt{\tfrac{1}{5}}v_{ssdd}^0 + v_{dsds}^2, \quad a_{02;0}^{(2)} = \tfrac{1}{3}v_{ssgg}^0 + v_{sgsg}^4,$$

$$a_{30;1}^{(2)} = -2\sqrt{\tfrac{1}{7}}v_{sddd}^2, \quad a_{21;0}^{(2)} = 2\sqrt{\tfrac{2}{7}}v_{sddg}^2 + \tfrac{6}{\sqrt{35}}v_{sgdd}^4,$$

$$a_{12;1}^{(2)} = -\tfrac{10}{3}\sqrt{\tfrac{2}{77}}v_{sdgg}^2 - 4\sqrt{\tfrac{5}{77}}v_{sgdg}^4, \quad a_{03;0}^{(2)} = -\tfrac{112}{9\sqrt{1001}}v_{sggg}^4,$$

$$a^{(2)}_{03;2} = -\frac{50}{9\sqrt{1001}}v^4_{sggg}, \quad a^{(2)}_{40;0} = \frac{1}{10}v^0_{dddd} + \frac{1}{7}v^2_{dddd} + \frac{9}{35}v^4_{dddd},$$

$$a^{(2)}_{31;1} = -\frac{2\sqrt{2}}{7}v^2_{dddg} - \frac{12}{7\sqrt{11}}v^4_{dddg},$$

$$a^{(2)}_{22;0} = \frac{1}{3\sqrt{5}}v^0_{ddgg} + \frac{5}{9}\sqrt{\frac{2}{11}}v^2_{ddgg} + \frac{16}{3\sqrt{715}}v^4_{ddgg}$$
$$+ \frac{2}{7}v^2_{dgdg} + \frac{1}{18}v^3_{dgdg} + \frac{85}{462}v^4_{dgdg} + \frac{47}{99}v^6_{dgdg},$$

$$a^{(2)}_{22;2} = \frac{5}{63}\sqrt{\frac{2}{11}}v^2_{ddgg} + \frac{10}{21}\sqrt{\frac{5}{143}}v^4_{ddgg} - \frac{1}{18}v^3_{dgdg} + \frac{5}{66}v^4_{dgdg} - \frac{2}{99}v^6_{dgdg},$$

$$a^{(2)}_{13;1} = -\frac{20}{21\sqrt{11}}v^2_{dggg} - \frac{36}{77}\sqrt{\frac{5}{13}}v^4_{dggg} - \frac{10\sqrt{2}}{33}v^6_{dggg},$$

$$a^{(2)}_{04;0} = \frac{1}{18}v^0_{gggg} + \frac{625}{6237}v^2_{gggg} + \frac{167}{2457}v^4_{gggg} + \frac{5}{81}v^6_{gggg} + \frac{2485}{11583}v^8_{gggg},$$

$$a^{(2)}_{04;2} = \frac{25}{891}v^2_{gggg} + \frac{50}{3861}v^4_{gggg} + \frac{35}{891}v^6_{gggg} + \frac{280}{11583}v^8_{gggg}, \tag{8}$$

in terms of the single-boson energies ϵ_ℓ and the matrix elements between normalized two-boson states,

$$v^L_{\ell_1\ell_2\ell'_1\ell'_2} \equiv \langle \ell_1\ell_2; LM|\hat{H}^{(2)}|\ell'_1\ell'_2; LM\rangle. \tag{9}$$

This analysis shows that the geometry of the sdg hamiltonian depends on 19 parameters (including E_0), considerably smaller than the 36 parameters of the quantum-mechanical version of the same hamiltonian. The structure of the phase diagram associated with the general sdg hamiltonian (7) might be of interest but is well beyond the scope of the present analysis. In the next section we show how a simplified sdg hamiltonian can be constructed which presumably captures the essential features of the phase-transitional behaviour in the sdg-IBM.

4. A generalized Casten triangle

A simplified hamiltonian of the sd-IBM is of the form

$$\hat{H}_{sd} = \epsilon_d\,\hat{n}_d + \kappa\,\hat{Q}\cdot\hat{Q} + \kappa'\hat{L}\cdot\hat{L}, \tag{10}$$

where $\hat{Q}$ is the quadrupole operator with components $\hat{Q}_\mu \equiv [d^\dagger\times\tilde{s}+s^\dagger\times\tilde{d}]^{(2)}_\mu+\chi[d^\dagger\times\tilde{d}]^{(2)}_\mu$ and $\hat{L}$ is the angular momentum operator, $\hat{L}_\mu \equiv \sqrt{10}\,[d^\dagger\times\tilde{d}]^{(1)}_\mu$. The $\hat{Q}^2$ and $\hat{L}^2$ terms in (10) constitute the hamiltonian of the so-called consistent-Q formalism (CQF) [47]; for $\chi = \pm\sqrt{7}/2$ it gives rise to the deformed or SU(3) limit and for $\chi = 0$ to the γ-unstable or SO(6) limit. In an extended consistent-Q formalism (ECQF) [48] the term $\hat{n}_d$ is added with which the third, vibrational or U(5) limit of the sd-IBM can be obtained. The ECQF hamiltonian thus allows one to reach all three limits of the model with four parameters.

The eigenfunctions of the ECQF hamiltonian are, in fact, independent of κ' and, furthermore, of the overall scale of the spectrum, reducing the number of essential parameters to two, the ratio κ/ϵ_d and χ. The physically relevant portion of this parameter space can be represented on a so-called Casten triangle [49]. Its vertices correspond to the three limits of the sd-IBM, U(5), SU(3) and SO(6) for spherical, deformed and γ-unstable nuclei, respectively. The three legs of the triangle describe

transitional cases, intermediate between two of the three limits, while an arbitrary point on the triangle corresponds to an admixture of the three limits.

In this paper we propose a similar hamiltonian in the *sdg*-IBM. The different dynamical symmetries of the *sdg*-IBM are known since long [50, 51]. In particular, three limits occur in *sdg*-IBM, namely U(5)⊗U(9), SU(3) and SO(15), that are the analogues of the limits of the *sd*-IBM. An immediate generalization of the *sd* hamiltonian (10) is therefore of the form

$$\hat{H}_{sdg} = \epsilon_d \hat{n}_d + \epsilon_g \hat{n}_g - \kappa \hat{Q}^{(2)} \cdot \hat{Q}^{(2)} - \kappa(1-\chi^2)\hat{Q}^{(4)} \cdot \hat{Q}^{(4)}, \tag{11}$$

where $\hat{Q}^{(2)}_\mu$ and $\hat{Q}^{(4)}_\mu$ are the quadrupole and hexadecapole operators, respectively, given by

$$\hat{Q}^{(2)}_\mu = \sigma[s^\dagger \times \tilde{d} + d^\dagger \times \tilde{s}]^{(2)}_\mu$$
$$+ \chi \left(\tfrac{11\sqrt{10}}{28}[d^\dagger \times \tilde{d}]^{(2)}_\mu - \tfrac{9}{7}\sigma'[d^\dagger \times \tilde{g} + g^\dagger \times \tilde{d}]^{(2)}_\mu + \tfrac{3\sqrt{55}}{14}[g^\dagger \times \tilde{g}]^{(2)}_\mu \right),$$
$$\hat{Q}^{(4)}_\mu = [s^\dagger \times \tilde{g} + g^\dagger \times \tilde{s}]^{(4)}_\mu. \tag{12}$$

The parameter χ is chosen so that $0 \leq \chi \leq 1$ and $\sigma, \sigma' = \pm 1$ are two arbitrary phases leading to four possible realizations of SU(3) [51]. For $\chi = 1$ the quadrupole operator is a generator of *sdg*-SU(3) while for $\chi = 0$ it becomes a generator of SO(15). Other parametrizations of the hexadecapole strength with the same effect could be taken in the hamiltonian (11), such as $\sqrt{1-\chi^2}$ or $(1 - |\chi|)$; they differ little in actual results and the dependence $(1 - \chi^2)$ is chosen here for its convenience. Note that with this parametrization the deformed limit has a vanishing hexadecapole interaction which is then only present in the γ-soft SO(15) limit. To do otherwise would require a hexadecapole operator taken from one of the other two strong coupling limits of *sdg*-IBM, SU(5) or SU(6). Since these have a questionable microscopic interpretation [52], this is not done here.

With the help of the expression (8) for the general hamiltonian of the *sdg*-IBM the classical limit of the special hamiltonian (11) yields

$$\frac{\langle \hat{H}_{sdg} \rangle}{N} = \frac{\epsilon_d \beta_2^2}{1 + \beta_2^2 + \beta_4^2} + \frac{\epsilon_g \beta_4^2}{1 + \beta_2^2 + \beta_4^2} - \frac{(N-1)\kappa}{(1 + \beta_2^2 + \beta_4^2)^2}$$
$$\times \left[4\beta_2^2 - \sigma\sigma'\chi \left(\tfrac{72}{7}\sqrt{\tfrac{2}{7}}\beta_2^2\beta_4 + \tfrac{2}{7}\sqrt{\tfrac{5}{7}}[11\beta_2^3 + 10\beta_2\beta_4^2]\sigma'\cos 3\gamma_2 \right) \right.$$
$$+ \chi^2 \left(\tfrac{605}{1372}\beta_2^4 + \tfrac{5813}{2058}\beta_2^2\beta_4^2 + \tfrac{3125}{6174}\beta_4^4 + \tfrac{18\sqrt{10}}{343}[11\beta_2^3\beta_4 \right.$$
$$\left. + 10\beta_2\beta_4^3]\sigma'\cos 3\gamma_2 - \tfrac{25}{6174}[33\beta_2^2\beta_4^2 + 35\beta_4^4]\cos 6\gamma_2 \right) \bigg]$$
$$- \frac{4(N-1)\kappa(1-\chi^2)\beta_4^2}{(1 + \beta_2^2 + \beta_4^2)^2}, \tag{13}$$

where only the two-body parts of the $\hat{Q}^{(2)} \cdot \hat{Q}^{(2)}$ and $\hat{Q}^{(4)} \cdot \hat{Q}^{(4)}$ operators have been considered. We note first of all that a change of sign of the product $\sigma\sigma'$ is equivalent with the change $\chi \rightarrow -\chi$. We may thus take $\sigma\sigma' = +1$ and consider the parameter range $-1 \leq \chi \leq +1$. Secondly, we remark that everywhere else σ' occurs in combination

with $\cos 3\gamma_2$ and, consequently, the change $\sigma' \to -\sigma'$ is equivalent with the replacement $\gamma_2 \to \pi/3 - \gamma_2$. This means that without loss of generality the choice $\sigma = \sigma' = +1$ can be made as long as the range $-1 \le \chi \le +1$ is considered. This can also be understood from the form of the $\hat{Q}_\mu^{(2)}$ operator in eq. (12) from which it is clear that the change $\sigma \to -\sigma$ is equivalent to $\chi \to -\chi$. The two choices $\chi = -1$ and $\chi = +1$ each correspond to a dynamical-symmetry limit of the SU(3) type which shall be referred to as $\mathrm{SU}_-(3)$ and $\mathrm{SU}_+(3)$, respectively.

Choosing ϵ_d as the overall energy scale, we summarize the preceding discussion by stating that we seek to minimize (in β_2, β_4 and γ_2) the following energy surface:

$$
\begin{aligned}
V_3&(\beta_2, \beta_4, \gamma_2; \eta, \chi, r) \\
={}& \frac{\beta_2^2}{1 + \beta_2^2 + \beta_4^2} + \frac{r\beta_4^2}{1 + \beta_2^2 + \beta_4^2} - \frac{\eta}{(1 + \beta_2^2 + \beta_4^2)^2} \\
& \times \left[4\beta_2^2 - \chi\left(\tfrac{72}{7}\sqrt{\tfrac{2}{7}}\beta_2^2\beta_4 + \tfrac{2}{7}\sqrt{\tfrac{5}{7}}[11\beta_2^3 + 10\beta_2\beta_4^2]\cos 3\gamma_2 \right) \right. \\
& \left. + \chi^2\left(\tfrac{605}{1372}\beta_2^4 + \tfrac{5813}{2058}\beta_2^2\beta_4^2 + \tfrac{3125}{6174}\beta_4^4 + \tfrac{18\sqrt{10}}{343}[11\beta_2^3\beta_4 \right. \right. \\
& \left. \left. + 10\beta_2\beta_4^3]\cos 3\gamma_2 - \tfrac{25}{6174}[33\beta_2^2\beta_4^2 + 35\beta_4^4]\cos 6\gamma_2 \right) \right] \\
& - \frac{4\eta(1 - \chi^2)\beta_4^2}{(1 + \beta_2^2 + \beta_4^2)^2},
\end{aligned}
\tag{14}
$$

where the notation $\eta \equiv (N-1)\kappa/\epsilon_d$ and $r \equiv \epsilon_g/\epsilon_d$ is introduced. The order parameters are β_2, β_4 and γ_2, and the control parameters are η, χ and r. The subscript 3 in V_3 refers to the number of order parameters and is used to distinguish it from V_2 introduced below. Physically meaningful values of the parameters imply $\eta > 0$. It is convenient to introduce, instead of $\eta = \xi/4(1 - \xi)$, the control parameter $\xi = 4\eta/(1 + 4\eta)$ such that $\xi \in [0, 1]$ instead of $\eta \in [0, +\infty[$. (The combination 4η instead of η is chosen in ξ for later convenience.) Furthermore, since the g boson is higher in energy than the d boson we have $r > 1$. In the limit $r \to \infty$ one recovers the sd-IBM. Again, it is more convenient to introduce, instead of $r = 1/(1 - \zeta)$, the control parameter $\zeta = (r - 1)/r$ such that $\zeta \in [0, 1]$ instead of $r \in [1, \infty[$. The definition adopted here for η or ξ is similar to the one of Iachello [6], so that we can easily compare with sd-IBM for $\zeta = 1$.

The parameter space covered by the hamiltonian (11) can be summarized with a generalization of the Casten triangle which becomes a prism, as shown in figure 1. Also indicated on the figure are the different symmetry limits of the sd-IBM and sdg-IBM. The point $(\xi, \zeta) = (0, 1)$ is denoted as U(5), as should be, and the point $(\xi, \zeta) = (0, 0)$, somewhat arbitrarily, as U(9), so that all vertices of the prism are labelled, facilitating the discussion of the structure of the phase diagram. Note that the U(5)⊗U(9) symmetry is valid for any combination of ϵ_d and ϵ_g (and hence for all $\zeta \in [0, 1]$) as long as $\xi = 0$.
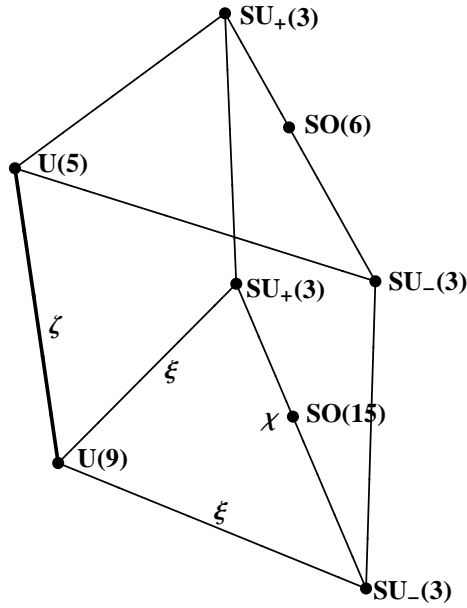
Figure 1. The Casten prism associated with the hamiltonian (11) of the *sdg*-IBM. The different symmetry limits of the *sd*-IBM and *sdg*-IBM are indicated with black dots. The three control parameters ξ, χ and ζ, as defined in the text, are indicated alongside the corresponding axes of the prism.

5. Method

The problem here is more complicated than in *sd*-IBM because of an extra order parameter (β_4) and an extra control parameter (r). The necessary and sufficient conditions for the potential energy V to have a (Morse or normal) critical point in $(\beta_2^*, \beta_4^*, \gamma_2^*)$ are

$$\left.\frac{\partial V_3}{\partial \beta_2}\right|_{(\beta_2^*,\beta_4^*,\gamma_2^*)} = \left.\frac{\partial V_3}{\partial \beta_4}\right|_{(\beta_2^*,\beta_4^*,\gamma_2^*)} = \left.\frac{\partial V_3}{\partial \gamma_2}\right|_{(\beta_2^*,\beta_4^*,\gamma_2^*)} = 0. \tag{15}$$

Furthermore, whether the critical point is a minimum, maximum or saddle point depends on whether the eigenvalues of the stability matrix in $(\beta_2^*, \beta_4^*, \gamma_2^*)$,

$$\mathcal{H}_3(\beta_2^*, \beta_4^*, \gamma_2^*; \xi, \chi, \zeta) \equiv \begin{bmatrix} \dfrac{\partial^2 V_3}{\partial \beta_2^2} & \dfrac{\partial^2 V_3}{\partial \beta_2 \partial \beta_4} & \dfrac{\partial^2 V_3}{\partial \beta_2 \partial \gamma_2} \\[2ex] \dfrac{\partial^2 V_3}{\partial \beta_4 \partial \beta_2} & \dfrac{\partial^2 V_3}{\partial \beta_4^2} & \dfrac{\partial^2 V_3}{\partial \beta_4 \partial \gamma_2} \\[2ex] \dfrac{\partial^2 V_3}{\partial \gamma_2 \partial \beta_2} & \dfrac{\partial^2 V_3}{\partial \gamma_2 \partial \beta_4} & \dfrac{\partial^2 V_3}{\partial \gamma_2^2} \end{bmatrix}_{(\beta_2^*,\beta_4^*,\gamma_2^*)}, \tag{16}$$

are all positive, all negative or both positive and negative. If, in addition to the condition (15), the determinant of the stability matrix vanishes,

$$\Delta_3(\beta_2^*, \beta_4^*, \gamma_2^*; \xi, \chi, \zeta) \equiv \det \mathcal{H}_3(\beta_2^*, \beta_4^*, \gamma_2^*; \xi, \chi, \zeta) = 0, \tag{17}$$

a so-called degenerate (or non-Morse) critical point is found [53]. This ensemble is of particular importance since it defines the points at which the energy surface changes in

structure and hence at which the system possibly undergoes a shape phase transition. The points that satisfy the condition (17) define a surface in the control parameters space (ξ, χ, ζ). Degenerate critical points shall be denoted as (ξ^*, χ^*, ζ^*). Our goal will be to determine the appearance of the degenerate critical surface in the Casten prism of figure 1.

The problem of determining the phase diagram for the Casten prism can be addressed by noting that solutions of the last of the equations in (15) satisfy one of the two equations

$$\sin 3\gamma_2 = 0, \qquad \cos 3\gamma_2 = \frac{9\beta_2(9\sqrt{2}\chi\beta_4 - 7\sqrt{7})(11\beta_2^2 + 10\beta_4^2)}{5\sqrt{5}\chi\beta_4^2(33\beta_2^2 + 35\beta_4^2)}. \tag{18}$$

These two conditions define the two possible classes of solutions. The *first class* corresponds to critical points with axial symmetry, $\gamma_2^* = 0$ (prolate) or $\gamma_2^* = \pi/3$ (oblate). A further simplification is then obtained by noting that the off-diagonal elements of the stability matrix involving γ_2 vanish at $\gamma_2^* = 0$ or $\gamma_2^* = \pi/3$, and hence the points in the degenerate critical set (ξ^*, χ^*, ζ^*) satisfy one of the two following equations:

$$\det \begin{bmatrix} \dfrac{\partial^2 V_3}{\partial \beta_2^2} & \dfrac{\partial^2 V_3}{\partial \beta_2 \partial \beta_4} \\[2ex] \dfrac{\partial^2 V_3}{\partial \beta_4 \partial \beta_2} & \dfrac{\partial^2 V_3}{\partial \beta_4^2} \end{bmatrix}_{(\beta_2^*, \beta_4^*, \gamma_2^*)} = 0, \qquad \left. \frac{\partial^2 V_3}{\partial \gamma_2^2} \right|_{(\beta_2^*, \beta_4^*, \gamma_2^*)} = 0. \tag{19}$$

Furthermore, we note that $\cos 3\gamma_2$ always occurs in Eq. (14) in combination with an odd power (1 or 3) of β_2. Since the replacement $\gamma_2 \to \pi/3 - \gamma_2$ corresponds to a change in sign of $\cos 3\gamma_2$ and no change in $\cos 6\gamma_2$, both cases $\gamma_2 = 0$ and $\gamma_2 = \pi/3$ are covered by putting $\gamma_2 = 0$ and allowing also negative values of β_2. This further simplifies the potential energy surface (14) which now only depends on the two order parameters β_2 and β_4,

$$\begin{aligned}
&V_2(\beta_2, \beta_4; \eta, \chi, r) \\
&= \frac{\beta_2^2}{1 + \beta_2^2 + \beta_4^2} + \frac{r\beta_4^2}{1 + \beta_2^2 + \beta_4^2} - \frac{\eta}{(1 + \beta_2^2 + \beta_4^2)^2} \\
&\quad \times \left[4\beta_2^2 + \chi\left(\frac{22}{7}\sqrt{\frac{5}{7}}\beta_2^3 + \frac{72}{7}\sqrt{\frac{2}{7}}\beta_2^2\beta_4 + \frac{20}{7}\sqrt{\frac{5}{7}}\beta_2\beta_4^2 \right) \right. \\
&\quad \left. + \chi^2\left(\frac{605}{1372}\beta_2^4 + \frac{198\sqrt{10}}{343}\beta_2^3\beta_4 + \frac{923}{343}\beta_2^2\beta_4^2 + \frac{180\sqrt{10}}{343}\beta_2\beta_4^3 + \frac{125}{343}\beta_4^4 \right) \right] \\
&\quad - \frac{4\eta(1 - \chi^2)\beta_4^2}{(1 + \beta_2^2 + \beta_4^2)^2}.
\end{aligned} \tag{20}$$

In summary, critical points (β_2^*, β_4^*) with axial symmetry are obtained from the simultaneous conditions

$$\left. \frac{\partial V_2}{\partial \beta_2} \right|_{(\beta_2^*, \beta_4^*)} = \left. \frac{\partial V_2}{\partial \beta_4} \right|_{(\beta_2^*, \beta_4^*)} = 0, \tag{21}$$

where one assumes $\gamma_2^* = 0$ and allows negative values of β_2^*. The points (ξ^*, χ^*, ζ^*) in the degenerate critical set should satisfy one of the two following equations:

$$\Delta_2(\beta_2^*, \beta_4^*; \xi, \chi, \zeta) = 0, \qquad \left.\frac{\partial^2 V_3}{\partial \gamma_2^2}\right|_{(\beta_2^*, \beta_4^*, \gamma_2^*)} = 0, \tag{22}$$

where $\Delta_2(\beta_2^*, \beta_4^*; \xi, \chi, \zeta)$ is the determinant of the 2×2 stability matrix,

$$\mathcal{H}_2(\beta_2^*, \beta_4^*; \xi, \chi, \zeta) \equiv \begin{bmatrix} \dfrac{\partial^2 V_2}{\partial \beta_2^2} & \dfrac{\partial^2 V_2}{\partial \beta_2 \partial \beta_4} \\ \dfrac{\partial^2 V_2}{\partial \beta_4 \partial \beta_2} & \dfrac{\partial^2 V_2}{\partial \beta_4^2} \end{bmatrix}_{(\beta_2^*, \beta_4^*)}. \tag{23}$$

The *second class* corresponds to critical points without axial symmetry, obtained as solutions of the second equation in (18).

Before attacking the problem of the occurrence of shape phase transitions for the entire hamiltonian (11), it is instructive to study, as a function of r or ζ, the three legs of the triangle between the limits $U(5) \otimes U(9)$, $SU_+(3)$ and $SU_-(3)$. This will determine the structure of the phase diagram on the faces of the prism of figure 1. In this analysis care should be taken to cover the two cases $\chi > 0$ and $\chi < 0$, and study in particular the behaviour at $\chi = 0$, for instance in the $SU_-(3)$–$SO(15)$–$SU_+(3)$ transition.

6. Partial phase diagrams

6.1. The U(5) ⊗ U(9) to SO(15) transition

The $U(5) \otimes U(9)$–$SO(15)$ transition is obtained for $\chi = 0$ and $r = 1$ (or $\zeta = 0$) while η varies from 0 to $+\infty$ (or ξ from 0 to 1). At the top side of the prism, for $r = \infty$ (or $\zeta = 1$), this reduces to the $U(5)$–$SO(6)$ transition. We are interested here in the entire phase diagram in η and r (or ξ and ζ) which can be established by an expansion in β_2 and β_4 around $(0,0)$. Since there is no dependence on γ_2 for $\chi = 0$, the analysis can be done starting from the potential (20). Up to fourth order we obtain

$$\begin{aligned} V_2(\beta_2, \beta_4; \eta, \chi = 0, r) \approx {} & (1 - 4\eta)\beta_2^2 + (r - 4\eta)\beta_4^2 - (1 - 8\eta)\beta_2^4 \\ & - (1 - 16\eta + r)\beta_2^2\beta_4^2 - (r - 8\eta)\beta_4^4, \end{aligned} \tag{24}$$

involving even powers of β_2 and β_4 only. The expansion (24) shows that the potential always exhibits a minimum, saddle point or maximum at $\beta_2^* = \beta_4^* = 0$. This is confirmed by computing the stability matrix at $\beta_2^* = \beta_4^* = 0$:

$$\mathcal{H}_2(0, 0; \xi, \chi = 0, \zeta) = \begin{bmatrix} \dfrac{2(1 - 2\xi)}{1 - \xi} & 0 \\ 0 & \dfrac{2[1 - \xi(2 - \zeta)]}{(1 - \xi)(1 - \zeta)} \end{bmatrix}. \tag{25}$$

The zeros of the determinant of the stability matrix determine the degenerate critical points which separate the different possible shapes of the potential. They are $\xi = 1/2$ (or $\eta = 1/4$) and $\xi = 1/(2 - \zeta)$ (or $\eta = r/4$). Consequently, we find that the potential

has (I) a minimum for $\xi < 1/2$, (IIa) a saddle point for $1/2 < \xi < 1/(2-\zeta)$ and (IIb) a maximum for $\xi > 1/(2-\zeta)$, always at $\beta_2^* = \beta_4^* = 0$.

In addition, for $\xi > 1/2$, critical points in β_2 occur for $\beta_2^* \neq 0$ (*i.e.* quadrupole-deformed critical points). The dependence of β_2^* on ξ and ζ is obtained by solving $\partial V_2/\partial \beta_2 = 0$ for $\beta_4 = 0$, yielding

$$\beta_2^* = \pm\sqrt{2\xi - 1} = \pm\sqrt{\frac{4 - \epsilon_d}{4 + \epsilon_d}}. \tag{26}$$

Hence the picture emerges that the spherical minimum $\beta_2^* = \beta_4^* = 0$ at $\xi = 1/2$ continuously evolves into the two quadrupole-deformed minima (26). The phase transition is of second order. It should be emphasized that this result is *independent* of ζ (or r) and that the entire line $\xi = 1/2$ exhibits a second-order phase transition when crossed. In particular, we recover the results of *sd*-IBM [6] which corresponds to $\zeta = 1$. One should verify the nature of the critical points by calculating the stability matrix at $\beta_2^* = \pm\sqrt{2\xi - 1}$ and $\beta_4^* = 0$:

$$\mathcal{H}_2(\pm\sqrt{2\xi - 1}, 0; \xi, \chi = 0, \zeta) = \begin{bmatrix} \dfrac{2\xi - 1}{2(1 - \xi)\xi^3} & 0 \\ 0 & \dfrac{\zeta}{\xi(1 - \zeta)} \end{bmatrix}. \tag{27}$$

Both matrix elements are positive definite and hence one always has a minimum.

Finally, for $\xi > 1/(2-\zeta)$, additional critical points with $\beta_4^* \neq 0$ occur (*i.e.* hexadecapole-deformed critical points). The dependence of β_4^* on ξ and ζ is obtained by solving $\partial V_2/\partial \beta_4 = 0$ for $\beta_2 = 0$, yielding

$$\beta_4^* = \pm\sqrt{\frac{\xi(2 - \zeta) - 1}{1 - \xi\zeta}} = \pm\sqrt{\frac{4 - \epsilon_g}{4 + \epsilon_g}}. \tag{28}$$

So the spherical saddle point $\beta_2^* = \beta_4^* = 0$ at $\xi = 1/(2-\zeta)$ continuously evolves into the two deformed critical points (28), the nature of which follows from the stability matrix at $\beta_2^* = 0$ and $\beta_4^* = \pm\sqrt{[\xi(2 - \zeta) - 1]/(1 - \xi\zeta)}$:

$$\mathcal{H}_2\left(0, \pm\sqrt{\frac{\xi(2 - \zeta) - 1}{1 - \xi\zeta}}; \xi, \chi = 0, \zeta\right)$$

$$= \begin{bmatrix} -\dfrac{\zeta(1 - \xi\zeta)}{\xi(1 - \zeta)^2} & 0 \\ 0 & \dfrac{[\xi(2 - \zeta) - 1](1 - \xi\zeta)^3}{2(1 - \xi)\xi^3(1 - \zeta)^4} \end{bmatrix}. \tag{29}$$

One matrix element is positive definite while the other is negative definite and hence both critical points are saddle points in this case.

The phase diagram in the (ξ, ζ) plane with $\chi = 0$ deduced in this way is shown in figure 2. The parameter space is divided in three areas with qualitatively different potentials in β_2 and β_4, characterized by the number and nature (minima, maxima or saddle) of Morse critical points. The potential surfaces in the regions indicated in figure 2 are characterized by
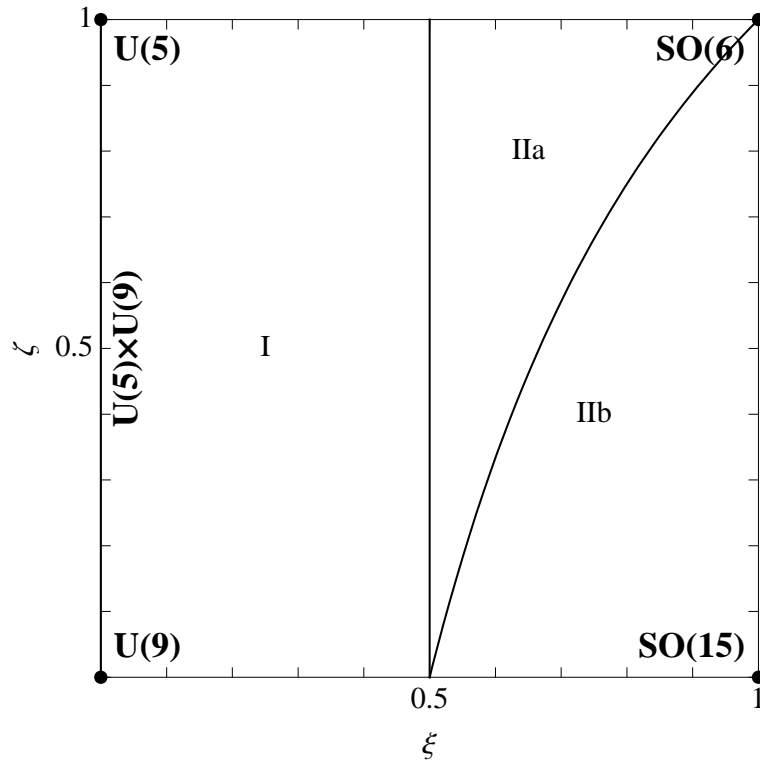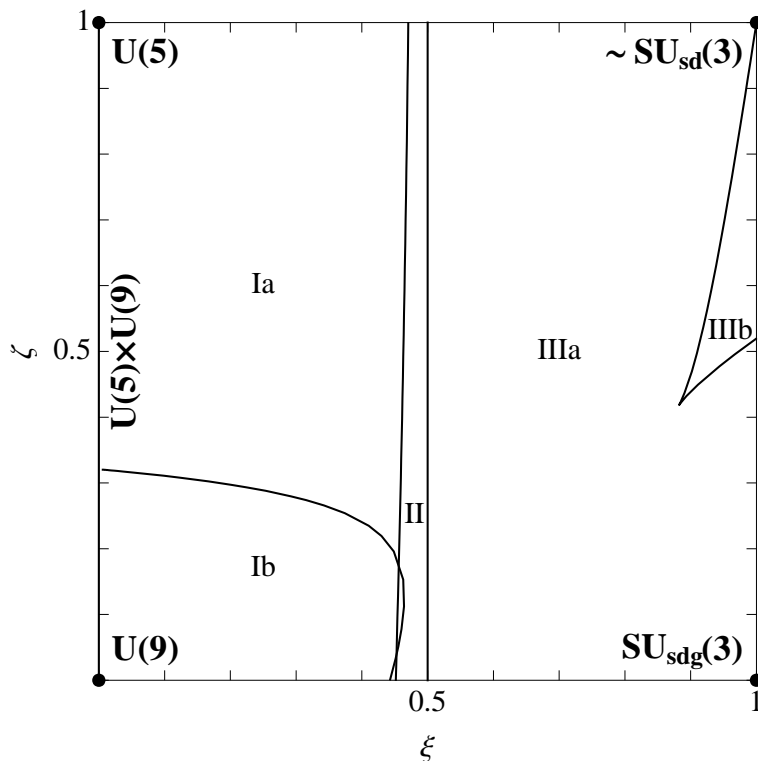
Figure 2. The phase diagram in the (ξ, ζ) plane of the Casten prism for $\chi = 0$. The lines or curves represent the locus of degenerate critical points that separate the different regions as discussed in the text. Symmetry limits of the *sd*-IBM and *sdg*-IBM are indicated with black dots. The entire ζ axis corresponds to the $U(5) \otimes U(9)$ limit of *sdg*-IBM.

- (I) a spherical minimum ($\beta_2^* = \beta_4^* = 0$);
- (IIa) a spherical saddle point and two quadrupole-deformed minima ($\beta_2^* \neq 0$, $\beta_4^* = 0$);
- (IIb) a spherical maximum, two quadrupole-deformed minima and two hexadecapole-deformed saddle points ($\beta_2^* = 0$, $\beta_4^* \neq 0$).

The degenerate critical lines in the phase diagram correspond to *bifurcation* lines: at $\xi = 1/2$ the spherical minimum splits into two quadrupole-deformed minima and at $\xi = 1/(2 - \zeta)$ the spherical saddle point splits into two hexadecapole-deformed saddle points.

6.2. The $U(5) \otimes U(9)$ to $SU(3)$ transitions

The $U(5) \otimes U(9)$–$SU_+(3)$ transition is obtained for $\chi = +1$ and $r = 1$ (or $\zeta = 0$) while η varies from 0 to $+\infty$ (or ξ from 0 to 1). A similar transition, from $U(5) \otimes U(9)$ to $SU_-(3)$, is obtained for $\chi = -1$. At the top side of the prism, for $r = \infty$ (or $\zeta = 1$), the $U(5) \otimes U(9)$–$SU_\pm(3)$ transitions almost reduce to $U(5)$–$SU_\pm(3)$, their analogues in *sd*-IBM. This correspondence is not exact since the coefficient of the $[d^\dagger \times \tilde{d}]_\mu^{(2)}$ term in

Figure 3. The phase diagram in the (ξ, ζ) plane of the Casten prism for $\chi = -1$. The lines or curves represent the locus of degenerate critical points with $\gamma_2^* = 0$ that separate the different regions as discussed in the text. Symmetry limits of the *sd*-IBM and *sdg*-IBM are indicated with black dots. The entire ζ axis corresponds to the $U(5) \otimes U(9)$ limit of *sdg*-IBM.

the quadrupole operator (12) is $11\sqrt{10}/28 \approx 1.24$ while it is $\sqrt{7}/2 \approx 1.32$ in *sd*-IBM. From the expression of the potential surface (14) we note that the change $\chi \rightarrow -\chi$ is equivalent to the simultaneous change $\beta_4 \rightarrow -\beta_4$ and $\gamma_2 \rightarrow \pi/3 - \gamma_2$. Hence all potential energy surfaces that can be realized for $\chi < 0$ follow from those with $\chi > 0$ and only one case needs to be studied. We are interested here in the entire phase diagram in η and r (or ξ and ζ) and consider the case $\chi = -1$.

An expansion up to third order around $(\beta_2, \beta_4) = (0, 0)$ gives

$$V(\beta_2, \beta_4, \gamma_2; \eta, \chi = -1, r) \approx (1 - 4\eta)\beta_2^2 + r\beta_4^2 - \tfrac{22}{7}\sqrt{\tfrac{5}{7}}\eta\beta_2^3 \cos 3\gamma_2$$
$$- \tfrac{72}{7}\sqrt{\tfrac{2}{7}}\eta\beta_2^2\beta_4 - \tfrac{20}{7}\sqrt{\tfrac{5}{7}}\eta\beta_2\beta_4^2 \cos 3\gamma_2. \qquad (30)$$

This shows that the spherical point $(\beta_2, \beta_4) = (0, 0)$ is always a minimum in β_4 since $r > 0$ and that it is a minimum in β_2 for $\xi < 1/2$ (or $\eta < 1/4$).

In general, critical points can only be obtained through a numerical solution of the equations (15) and (17), which, for a given χ, can be achieved as follows [with reference to the classical limit (13) expressed in units of $\kappa(N-1)$]. Since the hamiltonian is linear in ϵ_d and ϵ_g, it is straightforward to obtain as solutions of the first two equations in (15) analytic expressions $\epsilon_d(\beta_2, \beta_4)$ and $\epsilon_g(\beta_2, \beta_4)$. Furthermore, the solution of the third

equation in (15) is also known in closed form, see (18). As a result, the "unknowns" ϵ_d, ϵ_g and γ_2 can be eliminated from (17) to yield a single equation in β_2 and β_4. This equation cannot be solved analytically but, for a given value of β_2, and always for fixed given χ, a numerical solution in β_4 can be found, and from there γ_2, ϵ_d and ϵ_g are determined. Transforming from the $(\epsilon_d, \epsilon_g, \kappa(N-1))$ to the (ξ, ζ) variables, one thus finds parametric curves in (ξ, ζ) space with β_2 as parameter. Identical results are found by inverting the roles of β_2 and β_4, in which case the parametric curves in (ξ, ζ) space have β_4 as parameter.

The solution for $\chi = -1$ already displays a surprising richness which is illustrated in figure 3. The different curves in the figure represent the locus of degenerate critical points with $\gamma_2^* = 0$, that is, degenerate critical points that satisfy the first of the equations (18). The physical portion of the phase diagram with $0 \leq \xi \leq 1$ and $0 \leq \zeta \leq 1$ displays several regions distinguished by qualitatively different potentials. We may characterize a potential by listing all its critical points together with the signs of the eigenvalues of the stability matrix which distinguishes minima from maxima from saddle points. Hence we introduce for each critical point a notation $(\lambda_1, \lambda_2, \lambda_3)$ with $\lambda_i = \pm$. A minimum, for example, is denoted as $(+, +, +)$. A special situation arises for spherical critical points with $(\beta_2^*, \beta_4^*) = (0, 0)$ which can be characterized by the signs of the eigenvalues (λ_1, λ_2) of the 2×2 stability matrix (23). The different regions of figure 3 then have the following potentials:

- (Ia) $(+, +)$, $(+, -, -)$, $(-, -, -)$;
- (Ib) $(+, +)$, $(+, +, -)$, $(-, -, -)$;
- (II) $(+, +)$, $(+, +, +)$, $(+, +, -)$, $(+, -, -)$, $(-, -, -)$;
- (IIIa) $(+, -)$, $(+, +, +)$, $(+, +, -)$, $(+, -, -)$, $(-, -, -)$;
- (IIIb) $(+, -)$, $(+, +, +)$, $(+, +, -)$, $(+, -, -)^2$, $(-, -, -)^2$.

We emphasize that this is not the complete classification since it only concerns critical points with $\gamma_2^* = 0$; an even more complex diagram is found if solutions from the second of the equations (18) are included. In the study of phase transitions of quantum systems we are, however, primarily interested in the evolution of *global and local minima* of the potential. Therefore, we may for our purpose here ignore the evolution of saddle points and maxima, and concentrate on minima. From this point of view the phase diagram is divided into three regions characterized by potentials with (I) a spherical minimum, (II) a spherical and a deformed minimum, and (III) a deformed minimum. Also, if we confine our attention to the global and local minima of the potential only, no degenerate critical point with $\gamma_2 \neq 0$ is found to occur in the physical region of the phase diagram with $0 \leq \xi \leq 1$ and $0 \leq \zeta \leq 1$. From now on our analysis will be confined to the partition of the phase diagram into regions with potentials that differ in the properties of their minima.

The phase diagram for the U(5) $\otimes$ U(9)–SO(15) transition of subsection 6.1 is characterized by two main regions (I) and (II) (see figure 2) since (IIa) and (IIb) are distinguished by differences in saddle points and maxima only. With respect to the result
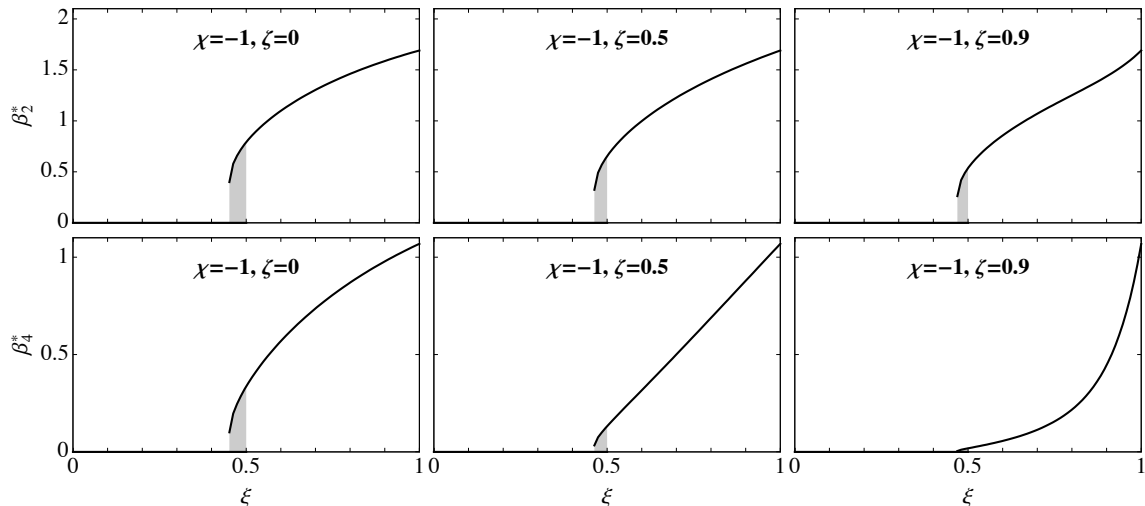
Figure 4. The evolution of the deformation parameters at equilibrium, β_2^* and β_4^*, along three different paths in the (ξ, ζ) plane with $0 \leq \xi \leq 1$ and $\zeta = 0$, 0.5 and 0.9, respectively. In each case the region of coexistence of a spherical and a deformed minimum is indicated by the grey area.

of subsection 6.1 we note that the $U(5) \otimes U(9)$–$SU(3)$ transition has an extra region (II) which is characterized by the coexistence of a spherical and a deformed minimum. This result is consistent with what is found in the *sd*-IBM and, moreover, we observe that, for realistic boson energies with $\epsilon_g > \epsilon_d$, the actual value of the g-boson energy has little influence on the size of the coexistence region.

Although one does not have analytic expressions for the deformation parameters at equilibrium, β_2^* and β_4^*, these can be obtained numerically and typical results are shown in figure 4 for three different paths in the (ξ, ζ) plane. The most striking evolution is that of the behaviour of β_4^* as a function of ζ. It is clear from the figure that a first-order transition occurs in β_4^* but the discontinuity in β_4^* becomes smaller for $\zeta \to 1$ (or $\epsilon_g \to \infty$).

6.3. The $SU_-(3)$–$SO(15)$–$SU_+(3)$ transition

The $SU_-(3)$–$SO(15)$–$SU_+(3)$ transition is obtained for $\eta = +\infty$ (or $\xi = 1$) while χ varies from -1 to $+1$. In the limit $\eta \to +\infty$ there is no dependence of the potential on either of the boson energies ϵ_d or ϵ_g, and hence the search for degenerate critical points is independent of ζ. It is easy to show that for $\chi = 0$ the equations (15) are satisfied for $\beta_2^{*2} + \beta_4^{*2} = 1$ and arbitrary γ_2^*. The potential is not only flat in γ_2 but in addition behaves like a Mexican hat in (β_2, β_4) around $(0,0)$. Furthermore, for $\beta_2^{*2} + \beta_4^{*2} = 1$, the condition (17) for a degenerate critical point is satisfied as well. Thus we find that all points with $\chi = 0$ and arbitrary ζ are degenerate critical. On this line the potential is flat in γ_2 and in the $SU_-(3)$–$SO(15)$–$SU_+(3)$ transition it tilts over from a prolate minimum with $\gamma_2^* = 0$ for $\chi < 0$ to an oblate one with $\gamma_2^* = \pi/3$ for $\chi > 0$. No other degenerate critical points occur for values of χ between -1 and $+1$.

7. The complete phase diagram

We are now in a position to piece together the entire phase diagram for $0 \leq \xi \leq 1$, $-1 \leq \chi \leq +1$ and $0 \leq \zeta \leq 1$. Since the change $\chi \to -\chi$ is equivalent to the simultaneous change $\beta_4 \to -\beta_4$ and $\gamma_2 \to \pi/3 - \gamma_2$, it is in fact sufficient to consider only positive or negative values of χ: the phase diagram is mirror-symmetric with respect to the U(5)–U(9)–SO(15)–SO(6) plane. In the following we consider the range $-1 \leq \chi \leq 0$.

An expansion of the potential up to third order,

$$V(\beta_2, \beta_4, \gamma_2; \eta, \chi, r) \approx (1 - 4\eta)\beta_2^2 + [r - 4\eta(1 - \chi^2)]\beta_4^2$$
$$+ \tfrac{22}{7}\sqrt{\tfrac{5}{7}}\chi\eta\beta_2^3\cos 3\gamma_2 + \tfrac{72}{7}\sqrt{\tfrac{2}{7}}\chi\eta\beta_2^2\beta_4 + \tfrac{20}{7}\sqrt{\tfrac{5}{7}}\chi\eta\beta_2\beta_4^2\cos 3\gamma_2, \quad (31)$$

or, alternatively, the expression for the stability matrix at $\beta_2^* = \beta_4^* = 0$,

$$\mathcal{H}_2(0,0;\xi,\chi=0,\zeta) = \begin{bmatrix} \dfrac{2(1-2\xi)}{1-\xi} & 0 \\ 0 & \dfrac{2\{1 - \xi[2 - \zeta - \chi^2(1-\zeta)]\}}{(1-\xi)(1-\zeta)} \end{bmatrix}, \quad (32)$$

shows that at the spherical point the potential has (I) a minimum for $\xi < 1/2$ (or $\eta < 1/4$), (IIa) a saddle point for $1/2 < \xi < 1/[2 - \zeta - \chi^2(1-\zeta)]$ [or $1/4 < \eta < r/(4 - 4\chi^2)$] and (IIb) a maximum for $\xi > 1/[2 - \zeta - \chi^2(1 - \zeta)]$ [or $\eta > r/(4 - 4\chi^2)$], always at $\beta_2^* = \beta_4^* = 0$. The situation is similar to the transitions discussed in subsection 6.1, with the only difference that now the separation line between the regions (IIa) and (IIb) depends on the value of χ while for the U(5) $\otimes$ U(9)–SO(15) transition we have $\chi = 0$. If we confine ourselves to an analysis of the properties of the *minima* of the potential, we may ignore the separation between (IIa) and (IIb) and treat them as a single region.

A locus of points of particular interest is defined by the condition that *two* eigenvalues of the stability matrix vanish. This is possible if there are at least two order parameters and at least three control parameters, as is the case presently, and leads to a catastrophe function of the type $D_{\pm 4}$ [53]. From the stability matrix (32) it is seen that this happens at $\beta_2^* = \beta_4^* = 0$ for $\xi = 1/2$ (or $\eta = 1/4$) and $\chi^2 = \zeta/(\zeta - 1)$ (or $\chi^2 = (\epsilon_d - \epsilon_g)/\epsilon_d$). The locus of $D_{\pm 4}$ catastrophes is represented by a curve in the (ξ, χ, ζ) space but it is entirely situated in the non-physical portion of this space (for $\epsilon_g \leq \epsilon_d$, *below* the Casten prism of figure 1) with the exception of the single point $\xi = 1/2$, $\chi = \zeta = 0$ which is half-way between U(9) and SO(15).

We therefore come to the conclusion that nothing spectacular happens within the Casten prism which, when it comes to the properties of *minima*, is divided by two surfaces in to three regions (see figure 5). The first surface is a plane obtained for $\xi = 1/2$, $-1 \leq \chi \leq 0$ and $0 \leq \zeta \leq 1$. The second is a parametric surface with parameters (β_2, χ) [or (β_4, χ)], constructed with the technique explained in subsection 6.2. This situation closely parallels what is obtained in *sd*-IBM and, moreover, it is seen from figure 5 that the size of the coexistence region is not greatly influenced by the ratio of boson energies ϵ_g/ϵ_d (or ζ). We want to emphasize, however, that this is not a trivial conclusion but that this result depends on our choice of hamiltonian and of the domain
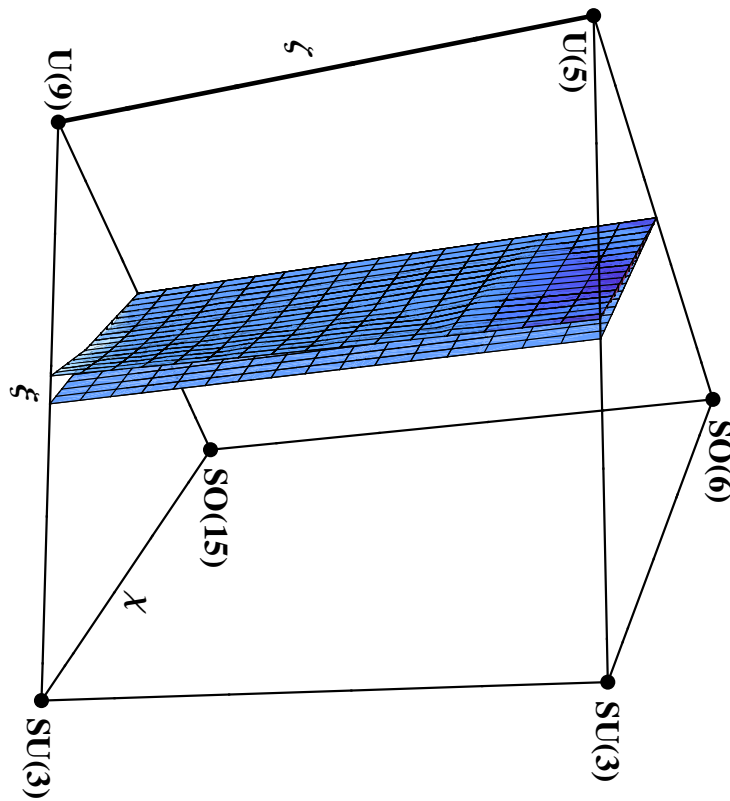
Figure 5. Phase diagram of the Casten prism associated with the hamiltonian (11) of the *sdg*-IBM. The two planes represent the locus of degenerate critical points that separate the spherical and deformed regions, and enclose the region of coexistence. The different symmetry limits of the *sd*-IBM and *sdg*-IBM are indicated with black dots.

available to the parameters ξ, χ and ζ which are guided by physics arguments. If we were to allow, for example, boson energies with $\epsilon_g < \epsilon_d$, a much more complex phase diagram would be uncovered which strongly departs from the one found in *sd*-IBM.

8. Conclusion

We summarize the three main assumptions at the basis of our geometric analysis of the *sdg*-IBM.

 (i) The general parametrization of a shape with quadrupole and hexadecapole deformation is reduced to one in terms of three variables $(\beta_2, \beta_4, \gamma_2)$.

 (ii) A simplified *sdg* hamiltonian is considered which is intermediate between four dynamical-symmetry limits of U(15), namely U(5) $\otimes$ U(9), SU$_\pm$(3) and SO(15).

 (iii) Parameters of this simplified *sdg* hamiltonian are restricted to physically acceptable values.

Under the above assumptions we find that the phase diagram is divided into three regions characterized by potentials with (I) a spherical minimum, (II) a spherical and a deformed minimum, and (III) a deformed minimum. The deformed minima are either prolate or oblate depending on the sign of the parameter χ in the quadrupole operator. No transition towards a stable triaxial shape is found.

Acknowledgments

9. References

[1] Gilmore R 1979 *J. Math. Phys.* **20** 891
[2] Arima A and Iachello F 1975 *Phys. Rev. Lett.* **35** 1069
[3] Arima A and Iachello F 1976 *Ann. Phys. (NY)* **99** 253
[4] Arima A and Iachello F 1978 *Ann. Phys. (NY)* **111** 201
[5] Arima A and Iachello F 1979 *Ann. Phys. (NY)* **123** 468
[6] Iachello F and Arima A 1987 *The Interacting Boson Model* (Cambridge: Cambridge University Press)
[7] Dieperink A E L, Scholten O and Iachello F 1980 *Phys. Rev. Lett.* **44** 1747
[8] Ginocchio J N and Kirson M W 1980 *Phys. Rev. Lett.* **44** 1744
[9] Bohr A and Mottelson B R 1980 *Phys. Scripta* **22** 468
[10] Bohr A and Mottelson B R 1975 *Nuclear Structure. II Nuclear Deformations* (Reading, Massachusetts: Benjamin)
[11] Feng D H, Gilmore R and S.R. Deans S R 1981 *Phys. Rev. C* **23** 1254
[12] López-Moreno E and Castaños O 1996 *Phys. Rev. C* **54** 2374
[13] Iachello F, Zamfir N V and Casten R F 1998 *Phys. Rev. Lett.* **81** 1191
[14] Casten R F, Kusnezov D and Zamfir N V 1999 *Phys. Rev. Lett.* **82** 5000
[15] Cejnar P and Jolie J 2000 *Phys. Rev. E* **61** 6237
[16] Iachello F 2000 *Phys. Rev. Lett.* **85** 3580
[17] Iachello F 2001 *Phys. Rev. Lett.* **87** 052502
[18] Casten R F and Zamfir N V 2000 *Phys. Rev. Lett.* **85** 3584
[19] Casten R F and Zamfir N V 2001 *Phys. Rev. Lett.* **87** 052503
[20] Frank A, Alonso C E and Arias J M, 2002 *Phys. Rev. C* **65** 014301
[21] Arias J M, Alonso C E, Vitturi A, García-Ramos J E, Dukelsky J and Frank A 2003 *Phys. Rev. C* **68** 041302(R)
[22] García-Ramos J E, Arias J M, Barea J and Frank A 2003 *Phys. Rev. C* **68** 024307
[23] Leviatan A and Ginocchio J N 2003 *Phys. Rev. Lett.* **90** 212501
[24] García-Ramos J E, Dukelsky J and Arias J M 2005 *Phys. Rev. C* **72** 037301
[25] Jolie J, Casten R F, von Brentano P and Werner V 2001 *Phys. Rev. Lett.* **78** 162501
[26] Jolie J and Linnemann A 2003 *Phys. Rev. C* **68** 031301(R)
[27] Jolie J, Cejnar P, Casten R F, Heinze S, Linnemann A and Werner V 2002 *Phys. Rev. Lett.* **89** 182502
[28] Cejnar P, Heinze S and Jolie J 2003 *Phys. Rev. C* **68** 034326
[29] Iachello F and Zamfir N V 2004 *Phys. Rev. Lett.* **92** 212501
[30] Cejnar P 2002 *Phys. Rev. C* **65** 044312
[31] Cejnar P 2003 *Phys. Rev. Lett.* **90** 112501

[32] Cejnar P and Jolie J 2004 *Phys. Rev. C* **69** 011301(R)
[33] Heyde K, Jolie J, Fossion R, De Baerdemacker S and Hellemans V 2004 *Phys. Rev. C* **69** 054304
[34] Rowe D J, Turner P S and Rosensteel G 2004 *Phys. Rev. Lett.* **93** 212502
[35] Rowe D J 2004 *Phys. Rev. Lett.* **93** 122502
[36] Rowe D J 2004 *Nucl. Phys. A* **745** 47
[37] Turner P S and Rowe D J 2005 *Nucl. Phys. A* **756** 333
[38] Rosensteel G and Rowe D J 2005 *Nucl. Phys. A* **759** 92
[39] Caprio M A, Cejnar P and Iachello F 2008 *Ann. Phys. (NY)* **323** 1106
[40] Caprio M A and Iachello F 2004 *Phys. Rev. Lett.* **93** 242502
[41] Frank A, Van Isacker P and Iachello F 2006 *Phys. Rev. C* **73** 061302(R)
[42] Devi Y D and Kota V K B 1992 *Pramana J. Phys.* **39** 413
[43] Devi Y D and Kota V K B 1990 *Z. Phys. A* **337** 15
[44] Rohoziński S G and Sobiczewski A 1981 *Acta Phys. Pol. B* **12** 1001
[45] Nazarewicz W and Rozmej P 1981 *Nucl. Phys. A* **369** 396
[46] Van Isacker P and Chen J-Q 1981 *Phys. Rev. C* **24** 684
[47] Warner D D and Casten R F 1982 *Phys. Rev. Lett.* **48** 1385
[48] Lipas P O, Toivonen P and Warner D D 1985 *Phys. Lett. B* **155** 295
[49] Casten R F 1981 *Interacting Bose-Fermi Systems in Nuclei*, edited by Iachello F (New York: Plenum) p 3
[50] Demeyer H, Van der Jeugt J, Vanden Berghe G and Kota V K B 1986 *J. Phys. A* **19** L565
[51] Kota V K B, Van der Jeugt J, Demeyer H and Vanden Berghe G 1987 *J. Math. Phys.* **28** 1644
[52] Bouldjedri A, Van Isacker P and Zerguine S 2005 *J. Phys. G* **31** 1329
[53] Gilmore R 1981 *Catastrophe Theory for Scientists and Engineers* (New York: Wiley)